



First Evidence for $B_s^0 \rightarrow \phi\phi$ Decay and Measurements of Branching Ratio and A_{CP} for
 $B^+ \rightarrow \phi K^+$

D. Acosta,¹⁶ J. Adelman,¹² T. Affolder,⁹ T. Akimoto,⁵⁴ M.G. Albrow,¹⁵ D. Ambrose,¹⁵ S. Amerio,⁴² D. Amidei,³³
A. Anastassov,⁵⁰ K. Anikeev,¹⁵ A. Annovi,⁴⁴ J. Antos,¹ M. Aoki,⁵⁴ G. Apollinari,¹⁵ T. Arisawa,⁵⁶ J-F. Arguin,³²
A. Artikov,¹³ W. Ashmanskas,¹⁵ A. Attal,⁷ F. Azfar,⁴¹ P. Azzi-Bacchetta,⁴² N. Bacchetta,⁴² H. Bachacou,²⁸
W. Badgett,¹⁵ A. Barbaro-Galtieri,²⁸ G.J. Barker,²⁵ V.E. Barnes,⁴⁶ B.A. Barnett,²⁴ S. Baroiant,⁶ G. Bauer,³¹
F. Bedeschi,⁴⁴ S. Behari,²⁴ S. Belforte,⁵³ G. Bellettini,⁴⁴ J. Bellinger,⁵⁸ A. Belloni,³¹ E. Ben-Haim,¹⁵ D. Benjamin,¹⁴
A. Beretvas,¹⁵ A. Bhatti,⁴⁸ M. Binkley,¹⁵ D. Bisello,⁴² M. Bishai,¹⁵ R.E. Blair,² C. Blocker,⁵ K. Bloom,³³
B. Blumenfeld,²⁴ A. Bocci,⁴⁸ A. Bodek,⁴⁷ G. Bolla,⁴⁶ A. Bolshov,³¹ D. Bortoletto,⁴⁶ J. Boudreau,⁴⁵ S. Bourov,¹⁵
B. Brau,⁹ C. Bromberg,³⁴ E. Brubaker,¹² J. Budagov,¹³ H.S. Budd,⁴⁷ K. Burkett,¹⁵ G. Busetto,⁴² P. Bussey,¹⁹
K.L. Byrum,² S. Cabrera,¹⁴ M. Campanelli,¹⁸ M. Campbell,³³ F. Canelli,⁷ A. Canepa,⁴⁶ M. Casarsa,⁵³
S. Castellano,⁴⁹ D. Carlsmith,⁵⁸ R. Carosi,⁴⁴ S. Carron,¹⁴ M. Cavalli-Sforza,³ A. Castro,⁴ P. Catastini,⁴⁴
D. Cauz,⁵³ A. Cerri,²⁸ L. Cerrito,⁴¹ J. Chapman,³³ Y.C. Chen,¹ M. Chertok,⁶ G. Chiarelli,⁴⁴ G. Chlachidze,¹³
F. Chlebana,¹⁵ I. Cho,²⁷ K. Cho,²⁷ D. Chokheli,¹³ J.P. Chou,²⁰ S. Chuang,⁵⁸ K. Chung,¹¹ W-H. Chung,⁵⁸
Y.S. Chung,⁴⁷ M. Cijliak,⁴⁴ C.I. Ciobanu,²³ M.A. Ciocci,⁴⁴ A.G. Clark,¹⁸ D. Clark,⁵ M. Coca,¹⁴ A. Connolly,²⁸
M. Convery,⁴⁸ J. Conway,⁶ B. Cooper,³⁰ K. Copic,³³ M. Cordelli,¹⁷ G. Cortiana,⁴² J. Cranshaw,⁵² J. Cuevas,¹⁰
A. Cruz,¹⁶ R. Culbertson,¹⁵ C. Currat,²⁸ D. Cyr,⁵⁸ D. Dagenhart,⁵ S. Da Ronco,⁴² S. D'Auria,¹⁹ P. de Barbaro,⁴⁷
S. De Cecco,⁴⁹ A. Deisher,²⁸ G. De Lentdecker,⁴⁷ M. Dell'Orso,⁴⁴ S. Demers,⁴⁷ L. Demortier,⁴⁸ M. Deninno,⁴
D. De Pedis,⁴⁹ P.F. Derwent,¹⁵ C. Dionisi,⁴⁹ J.R. Dittmann,¹⁵ P. DiTuro,⁵⁰ C. Dörr,²⁵ A. Dominguez,²⁸
S. Donati,⁴⁴ M. Donega,¹⁸ J. Donini,⁴² M. D'Onofrio,¹⁸ T. Dorigo,⁴² K. Ebina,⁵⁶ J. Efron,³⁸ J. Ehlers,¹⁸
R. Erbacher,⁶ M. Erdmann,²⁵ D. Errede,²³ S. Errede,²³ R. Eusebi,⁴⁷ H-C. Fang,²⁸ S. Farrington,²⁹
I. Fedorko,⁴⁴ W.T. Fedorko,¹² R.G. Feild,⁵⁹ M. Feindt,²⁵ J.P. Fernandez,⁴⁶ R.D. Field,¹⁶ G. Flanagan,³⁴
B. Flaughner,¹⁵ L.R. Flores-Castillo,⁴⁵ A. Foland,²⁰ S. Forrester,⁶ G.W. Foster,¹⁵ M. Franklin,²⁰ J.C. Freeman,²⁸
Y. Fujii,²⁶ I. Furic,¹² A. Gajjar,²⁹ J. Galyardt,¹¹ M. Gallinaro,⁴⁸ M. Garcia-Sciveres,²⁸ A.F. Garfinkel,⁴⁶
C. Gay,⁵⁹ H. Gerberich,¹⁴ D.W. Gerdes,³³ E. Gerchtein,¹¹ S. Giagu,⁴⁹ P. Giannetti,⁴⁴ A. Gibson,²⁸
K. Gibson,¹¹ C. Ginsburg,¹⁵ K. Giolo,⁴⁶ M. Giordani,⁵³ M. Giunta,⁴⁴ G. Giurgiu,¹¹ V. Glagolev,¹³
D. Glenzinski,¹⁵ M. Gold,³⁶ N. Goldschmidt,³³ D. Goldstein,⁷ J. Goldstein,⁴¹ G. Gomez,¹⁰ G. Gomez-Ceballos,¹⁰
M. Goncharov,⁵¹ O. González,⁴⁶ I. Gorelov,³⁶ A.T. Goshaw,¹⁴ Y. Gotra,⁴⁵ K. Goulianos,⁴⁸ A. Gresele,⁴²
M. Griffiths,²⁹ C. Grosso-Pilcher,¹² U. Grundler,²³ J. Guimaraes da Costa,²⁰ C. Haber,²⁸ K. Hahn,⁴³ S.R. Hahn,¹⁵
E. Halkiadakis,⁴⁷ A. Hamilton,³² B-Y. Han,⁴⁷ R. Handler,⁵⁸ F. Happacher,¹⁷ K. Hara,⁵⁴ M. Hare,⁵⁵ R.F. Harr,⁵⁷
R.M. Harris,¹⁵ F. Hartmann,²⁵ K. Hatakeyama,⁴⁸ J. Hauser,⁷ C. Hays,¹⁴ H. Hayward,²⁹ B. Heinemann,²⁹
J. Heinrich,⁴³ M. Hennecke,²⁵ M. Herndon,²⁴ C. Hill,⁹ D. Hirschbuehl,²⁵ A. Hocker,¹⁵ K.D. Hoffman,¹²
A. Holloway,²⁰ S. Hou,¹ M.A. Houlden,²⁹ B.T. Huffman,⁴¹ Y. Huang,¹⁴ R.E. Hughes,³⁸ J. Huston,³⁴ K. Ikado,⁵⁶
J. Incandela,⁹ G. Introzzi,⁴⁴ M. Iori,⁴⁹ Y. Ishizawa,⁵⁴ C. Issever,⁹ A. Ivanov,⁶ Y. Iwata,²² B. Iyutin,³¹ E. James,¹⁵
D. Jang,⁵⁰ B. Jayatilaka,³³ D. Jeans,⁴⁹ H. Jensen,¹⁵ E.J. Jeon,²⁷ M. Jones,⁴⁶ K.K. Joo,²⁷ S.Y. Jun,¹¹ T. Junk,²³
T. Kamon,⁵¹ J. Kang,³³ M. Karagoz Unel,³⁷ P.E. Karchin,⁵⁷ Y. Kato,⁴⁰ Y. Kemp,²⁵ R. Kephart,¹⁵ U. Kerzel,²⁵
V. Khotilovich,⁵¹ B. Kilminster,³⁸ D.H. Kim,²⁷ H.S. Kim,²³ J.E. Kim,²⁷ M.J. Kim,¹¹ M.S. Kim,²⁷ S.B. Kim,²⁷
S.H. Kim,⁵⁴ Y.K. Kim,¹² M. Kirby,¹⁴ L. Kirsch,⁵ S. Klimenko,¹⁶ B. Knuteson,³¹ B.R. Ko,¹⁴ H. Kobayashi,⁵⁴
D.J. Kong,²⁷ K. Kondo,⁵⁶ J. Konigsberg,¹⁶ K. Kordas,³² A. Korn,³¹ A. Korytov,¹⁶ A.V. Kotwal,¹⁴ A. Kovalev,⁴³
J. Kraus,²³ I. Kravchenko,³¹ A. Kreymer,¹⁵ J. Kroll,⁴³ M. Kruse,¹⁴ V. Krutelyov,⁵¹ S.E. Kuhlmann,² S. Kwang,¹²
A.T. Laasanen,⁴⁶ S. Lai,³² S. Lami,^{44,48} S. Lammel,¹⁵ M. Lancaster,³⁰ R. Lander,⁶ K. Lannon,³⁸ A. Lath,⁵⁰
G. Latino,⁴⁴ R. Lauhakangas,²¹ I. Lazzizzera,⁴² C. Lecci,²⁵ T. LeCompte,² J. Lee,²⁷ J. Lee,⁴⁷ S.W. Lee,⁵¹
R. Lefèvre,³ N. Leonardo,³¹ S. Leone,⁴⁴ S. Levy,¹² J.D. Lewis,¹⁵ K. Li,⁵⁹ C. Lin,⁵⁹ C.S. Lin,¹⁵ M. Lindgren,¹⁵
E. Lipeles,⁸ T.M. Liss,²³ A. Lister,¹⁸ D.O. Litvintsev,¹⁵ T. Liu,¹⁵ Y. Liu,¹⁸ N.S. Lockyer,⁴³ A. Logunov,³⁵
M. Loretì,⁴² P. Loverre,⁴⁹ R-S. Lu,¹ D. Lucchesi,⁴² P. Lujan,²⁸ P. Lukens,¹⁵ G. Lungu,¹⁶ L. Lyons,⁴¹ J. Lys,²⁸
R. Lysak,¹ E. Lytken,⁴⁶ D. MacQueen,³² R. Madrak,¹⁵ K. Maeshima,¹⁵ P. Maksimovic,²⁴ N. Maladinovic,⁵
G. Manca,²⁹ R. Marginean,¹⁵ C. Marino,²³ A. Martin,⁵⁹ M. Martin,²⁴ V. Martin,³⁷ M. Martínez,³ T. Maruyama,⁵⁴
H. Matsunaga,⁵⁴ M. Mattson,⁵⁷ P. Mazzanti,⁴ K.S. McFarland,⁴⁷ D. McGivern,³⁰ P.M. McIntyre,⁵¹ P. McNamara,⁵⁰
A. Mehta,²⁹ S. Menzemer,³¹ A. Menzione,⁴⁴ P. Merkel,⁴⁶ C. Mesropian,⁴⁸ A. Messina,⁴⁹ T. Miao,¹⁵ J. Miles,³¹
L. Miller,²⁰ R. Miller,³⁴ J.S. Miller,³³ C. Mills,⁹ R. Miquel,²⁸ S. Miscetti,¹⁷ G. Mitselmakher,¹⁶ A. Miyamoto,²⁶

N. Moggi,⁴ B. Mohr,⁷ R. Moore,¹⁵ M. Morello,⁴⁴ P.A. Movilla Fernandez,²⁸ J. Muelmenstaedt,²⁸ A. Mukherjee,¹⁵ M. Mulhearn,³¹ T. Muller,²⁵ R. Mumford,²⁴ A. Munar,⁴³ P. Murat,¹⁵ J. Nachtman,¹⁵ S. Nahn,⁵⁹ I. Nakano,³⁹ A. Napier,⁵⁵ R. Napora,²⁴ D. Naumov,³⁶ V. Necula,¹⁶ J. Nielsen,²⁸ T. Nelson,¹⁵ C. Neu,⁴³ M.S. Neubauer,⁸ T. Nigmanov,⁴⁵ L. Nodulman,² O. Norriella,³ T. Ogawa,⁵⁶ S.H. Oh,¹⁴ Y.D. Oh,²⁷ T. Ohsugi,²² T. Okusawa,⁴⁰ R. Oldeman,²⁹ R. Orava,²¹ W. Orejudos,²⁸ K. Osterberg,²¹ C. Pagliarone,⁴⁴ E. Palencia,¹⁰ R. Paoletti,⁴⁴ V. Papadimitriou,¹⁵ A.A. Paramonov,¹² S. Pashapour,³² J. Patrick,¹⁵ G. Pauletta,⁵³ M. Paulini,¹¹ C. Paus,³¹ D. Pellett,⁶ A. Penzo,⁵³ T.J. Phillips,¹⁴ G. Piacentino,⁴⁴ J. Piedra,¹⁰ K.T. Pitts,²³ C. Plager,⁷ L. Pondrom,⁵⁸ G. Pope,⁴⁵ X. Portell,³ O. Poukhov,¹³ N. Pounder,⁴¹ F. Prakoshyn,¹³ T. Pratt,²⁹ A. Pronko,¹⁶ J. Proudfoot,² F. Ptohos,¹⁷ G. Punzi,⁴⁴ J. Rademacker,⁴¹ M.A. Rahaman,⁴⁵ A. Rakitine,³¹ S. Rappoccio,²⁰ F. Ratnikov,⁵⁰ H. Ray,³³ B. Reisert,¹⁵ V. Rekovic,³⁶ P. Renton,⁴¹ M. Rescigno,⁴⁹ F. Rimondi,⁴ K. Rinnert,²⁵ L. Ristori,⁴⁴ W.J. Robertson,¹⁴ A. Robson,¹⁹ T. Rodrigo,¹⁰ S. Rolli,⁵⁵ R. Roser,¹⁵ R. Rossin,¹⁶ C. Rott,⁴⁶ J. Russ,¹¹ V. Rusu,¹² A. Ruiz,¹⁰ D. Ryan,⁵⁵ H. Saarikko,²¹ S. Sabik,³² A. Safonov,⁶ R. St. Denis,¹⁹ W.K. Sakumoto,⁴⁷ G. Salamanna,⁴⁹ D. Saltzberg,⁷ C. Sanchez,³ L. Santi,⁵³ S. Sarkar,⁴⁹ K. Sato,⁵⁴ P. Savard,³² A. Savoy-Navarro,¹⁵ P. Schlabach,¹⁵ E.E. Schmidt,¹⁵ M.P. Schmidt,⁵⁹ M. Schmitt,³⁷ L. Scodellaro,¹⁰ A.L. Scott,⁹ A. Scribano,⁴⁴ F. Scuri,⁴⁴ A. Sedov,⁴⁶ S. Seidel,³⁶ Y. Seiya,⁴⁰ A. Semenov,¹³ F. Semeria,⁴ L. Sexton-Kennedy,¹⁵ I. Sfiligoi,¹⁷ M.D. Shapiro,²⁸ T. Shears,²⁹ P.F. Shepard,⁴⁵ D. Sherman,²⁰ M. Shimojima,⁵⁴ M. Shochet,¹² Y. Shon,⁵⁸ I. Shreyber,³⁵ A. Sidoti,⁴⁴ A. Sill,⁵² P. Sinervo,³² A. Sisakyan,¹³ J. Sjolín,⁴¹ A. Skiba,²⁵ A.J. Slaughter,¹⁵ K. Sliwa,⁵⁵ D. Smirnov,³⁶ J.R. Smith,⁶ F.D. Snider,¹⁵ R. Snihur,³² M. Soderberg,³³ A. Soha,⁶ S.V. Somalwar,⁵⁰ J. Spalding,¹⁵ M. Spezziga,⁵² F. Spinella,⁴⁴ P. Squillacioti,⁴⁴ H. Stadie,²⁵ M. Stanitzki,⁵⁹ B. Stelzer,³² O. Stelzer-Chilton,³² D. Stentz,³⁷ J. Strologas,³⁶ D. Stuart,⁹ J. S. Suh,²⁷ A. Sukhanov,¹⁶ K. Sumorok,³¹ H. Sun,⁵⁵ T. Suzuki,⁵⁴ A. Taffard,²³ R. Tafirout,³² H. Takano,⁵⁴ R. Takashima,³⁹ Y. Takeuchi,⁵⁴ K. Takikawa,⁵⁴ M. Tanaka,² R. Tanaka,³⁹ N. Tanimoto,³⁹ M. Tecchio,³³ P.K. Teng,¹ K. Terashi,⁴⁸ R.J. Tesarek,¹⁵ S. Tether,³¹ J. Thom,¹⁵ A.S. Thompson,¹⁹ E. Thomson,⁴³ P. Tipton,⁴⁷ V. Tiwari,¹¹ S. Tkaczyk,¹⁵ D. Toback,⁵¹ K. Tollefson,³⁴ T. Tomura,⁵⁴ D. Tonelli,⁴⁴ M. Tönnemann,³⁴ S. Torre,⁴⁴ D. Torretta,¹⁵ S. Tourneur,¹⁵ W. Trischuk,³² R. Tsuchiya,⁵⁶ S. Tsuno,³⁹ D. Tsybychev,¹⁶ N. Turini,⁴⁴ F. Ukegawa,⁵⁴ T. Unverhau,¹⁹ S. Uozumi,⁵⁴ D. Usynin,⁴³ L. Vacavant,²⁸ A. Vaiciulis,⁴⁷ A. Varganov,³³ S. Vejck III,¹⁵ G. Velev,¹⁵ V. Veszpremi,⁴⁶ G. Veramendi,²³ T. Vickey,²³ R. Vidal,¹⁵ I. Vila,¹⁰ R. Vilar,¹⁰ I. Vollrath,³² I. Volobouev,²⁸ M. von der Mey,⁷ P. Wagner,⁵¹ R.G. Wagner,² R.L. Wagner,¹⁵ W. Wagner,²⁵ R. Wallny,⁷ T. Walter,²⁵ Z. Wan,⁵⁰ M.J. Wang,¹ S.M. Wang,¹⁶ A. Warburton,³² B. Ward,¹⁹ S. Waschke,¹⁹ D. Waters,³⁰ T. Watts,⁵⁰ M. Weber,²⁸ W.C. Wester III,¹⁵ B. Whitehouse,⁵⁵ D. Whiteson,⁴³ A.B. Wicklund,² E. Wicklund,¹⁵ H.H. Williams,⁴³ P. Wilson,¹⁵ B.L. Winer,³⁸ P. Wittich,⁴³ S. Wolbers,¹⁵ C. Wolfe,¹² M. Wolter,⁵⁵ M. Worcester,⁷ S. Worm,⁵⁰ T. Wright,³³ X. Wu,¹⁸ F. Würthwein,⁸ A. Wyatt,³⁰ A. Yagil,¹⁵ T. Yamashita,³⁹ K. Yamamoto,⁴⁰ J. Yamaoka,⁵⁰ C. Yang,⁵⁹ U.K. Yang,¹² W. Yao,²⁸ G.P. Yeh,¹⁵ J. Yoh,¹⁵ K. Yorita,⁵⁶ T. Yoshida,⁴⁰ I. Yu,²⁷ S. Yu,⁴³ J.C. Yun,¹⁵ L. Zanello,⁴⁹ A. Zanetti,⁵³ I. Zaw,²⁰ F. Zetti,⁴⁴ J. Zhou,⁵⁰ and S. Zucchelli⁴

(CDF Collaboration)

¹*Institute of Physics, Academia Sinica, Taipei, Taiwan 11529, Republic of China*

²*Argonne National Laboratory, Argonne, Illinois 60439*

³*Institut de Física d'Altes Energies, Universitat Autònoma de Barcelona, E-08193, Bellaterra (Barcelona), Spain*

⁴*Istituto Nazionale di Fisica Nucleare, University of Bologna, I-40127 Bologna, Italy*

⁵*Brandeis University, Waltham, Massachusetts 02254*

⁶*University of California at Davis, Davis, California 95616*

⁷*University of California at Los Angeles, Los Angeles, California 90024*

⁸*University of California at San Diego, La Jolla, California 92093*

⁹*University of California at Santa Barbara, Santa Barbara, California 93106*

¹⁰*Instituto de Física de Cantabria, CSIC-University of Cantabria, 39005 Santander, Spain*

¹¹*Carnegie Mellon University, Pittsburgh, PA 15213*

¹²*Enrico Fermi Institute, University of Chicago, Chicago, Illinois 60637*

¹³*Joint Institute for Nuclear Research, RU-141980 Dubna, Russia*

¹⁴*Duke University, Durham, North Carolina 27708*

¹⁵*Fermi National Accelerator Laboratory, Batavia, Illinois 60510*

¹⁶*University of Florida, Gainesville, Florida 32611*

¹⁷*Laboratori Nazionali di Frascati, Istituto Nazionale di Fisica Nucleare, I-00044 Frascati, Italy*

¹⁸*University of Geneva, CH-1211 Geneva 4, Switzerland*

¹⁹*Glasgow University, Glasgow G12 8QQ, United Kingdom*

²⁰*Harvard University, Cambridge, Massachusetts 02138*

²¹Division of High Energy Physics, Department of Physics,
University of Helsinki and Helsinki Institute of Physics, FIN-00044, Helsinki, Finland

²²Hiroshima University, Higashi-Hiroshima 724, Japan

²³University of Illinois, Urbana, Illinois 61801

²⁴The Johns Hopkins University, Baltimore, Maryland 21218

²⁵Institut für Experimentelle Kernphysik, Universität Karlsruhe, 76128 Karlsruhe, Germany

²⁶High Energy Accelerator Research Organization (KEK), Tsukuba, Ibaraki 305, Japan

²⁷Center for High Energy Physics: Kyungpook National University, Taegu 702-701; Seoul National University,
Seoul 151-742; and SungKyunKwan University, Suwon 440-746; Korea

²⁸Ernest Orlando Lawrence Berkeley National Laboratory, Berkeley, California 94720

²⁹University of Liverpool, Liverpool L69 7ZE, United Kingdom

³⁰University College London, London WC1E 6BT, United Kingdom

³¹Massachusetts Institute of Technology, Cambridge, Massachusetts 02139

³²Institute of Particle Physics: McGill University, Montréal,
Canada H3A 2T8; and University of Toronto, Toronto, Canada M5S 1A7

³³University of Michigan, Ann Arbor, Michigan 48109

³⁴Michigan State University, East Lansing, Michigan 48824

³⁵Institution for Theoretical and Experimental Physics, ITEP, Moscow 117259, Russia

³⁶University of New Mexico, Albuquerque, New Mexico 87131

³⁷Northwestern University, Evanston, Illinois 60208

³⁸The Ohio State University, Columbus, Ohio 43210

³⁹Okayama University, Okayama 700-8530, Japan

⁴⁰Osaka City University, Osaka 588, Japan

⁴¹University of Oxford, Oxford OX1 3RH, United Kingdom

⁴²University of Padova, Istituto Nazionale di Fisica Nucleare,
Sezione di Padova-Trento, I-35131 Padova, Italy

⁴³University of Pennsylvania, Philadelphia, Pennsylvania 19104

⁴⁴Istituto Nazionale di Fisica Nucleare Pisa, Universities of Pisa,
Siena and Scuola Normale Superiore, I-56127 Pisa, Italy

⁴⁵University of Pittsburgh, Pittsburgh, Pennsylvania 15260

⁴⁶Purdue University, West Lafayette, Indiana 47907

⁴⁷University of Rochester, Rochester, New York 14627

⁴⁸The Rockefeller University, New York, New York 10021

⁴⁹Istituto Nazionale di Fisica Nucleare, Sezione di Roma 1,
University di Roma "La Sapienza," I-00185 Roma, Italy

⁵⁰Rutgers University, Piscataway, New Jersey 08855

⁵¹Texas A&M University, College Station, Texas 77843

⁵²Texas Tech University, Lubbock, Texas 79409

⁵³Istituto Nazionale di Fisica Nucleare, University of Trieste/ Udine, Italy

⁵⁴University of Tsukuba, Tsukuba, Ibaraki 305, Japan

⁵⁵Tufts University, Medford, Massachusetts 02155

⁵⁶Waseda University, Tokyo 169, Japan

⁵⁷Wayne State University, Detroit, Michigan 48201

⁵⁸University of Wisconsin, Madison, Wisconsin 53706

⁵⁹Yale University, New Haven, Connecticut 06520

(Dated: February 20, 2005)

We present the first evidence for the decay $B_s^0 \rightarrow \phi\phi$ and a measurement of the Branching Ratio $\text{BR}(B_s^0 \rightarrow \phi\phi)$ using 180 pb^{-1} of data collected by the CDF II experiment at the Fermilab Tevatron collider. In addition, the BR and direct CP asymmetry for the $B^+ \rightarrow \phi K^+$ decay are measured. We obtain: $\text{BR}(B_s^0 \rightarrow \phi\phi) = (14_{-5}^{+6}(\text{stat.}) \pm 6(\text{syst.})) \times 10^{-6}$, $\text{BR}(B^+ \rightarrow \phi K^+) = (7.6 \pm 1.3(\text{stat.}) \pm 0.6(\text{syst.})) \times 10^{-6}$, and $A_{CP}(B^+ \rightarrow \phi K^+) = -0.07 \pm 0.17(\text{stat.})_{-0.02}^{+0.03}(\text{syst.})$. Both decays are governed in the Standard Model by second order (penguin) $b \rightarrow s\bar{s}s$ amplitudes.

PACS numbers: 13.25.Hw 14.40.Nd

Recent measurements [1, 2] of CP asymmetries for $B^0 \rightarrow \phi K_S^0$ and $B^0 \rightarrow \eta' K_S^0$ suggest deviation from Standard Model (SM) predictions in B meson decays involving $b \rightarrow s\bar{s}s$ transitions, which also generate both $B_s^0 \rightarrow \phi\phi$ and $B^+ \rightarrow \phi K^+$ decays. Charmless B_s^0 to Vector-Vector decays have not yet been observed. These modes

are of special interest because the angular correlations in the final state allow the separation of CP -even and odd components of the decay amplitude. With sufficient statistics, measurements of the decay width difference ($\Delta\Gamma_s$) and of CKM parameters and tests of the predictions for polarizations will be possible [3]. In particular

the $B_s^0 \rightarrow \phi\phi$ decay has been considered as a probe for New Physics scenarios [4] recently advocated to explain the apparent deviations. Recent calculations predict a branching ratio $\text{BR}(B_s^0 \rightarrow \phi\phi)$ between 10×10^{-6} [5] and 37×10^{-6} [6]. Within the SM the $B^+ \rightarrow \phi K^+$ direct CP asymmetry (A_{CP}) is predicted not to exceed a few percent level [7]. No single experiment [8] has yet reached the sensitivity to detect this asymmetry. Further measurements of decay rates and A_{CP} may help identifying the source of the apparent deviations from SM predictions in $b \rightarrow s\bar{s}s$ penguin dominated B decays.

We report the first evidence of $B_s^0 \rightarrow \phi\phi$ decays, and present the first measurements of the CP -averaged BR and A_{CP} for $B^+ \rightarrow \phi K^+$ [9] at hadron colliders. To cancel the uncertainty in the B hadron production cross section and to reduce systematic uncertainties on detector efficiencies, the branching fractions are extracted from ratios of the decay rates of interest normalized to the established $B_s^0 \rightarrow J/\psi\phi$ and $B^+ \rightarrow J/\psi K^+$ decay modes, which are characterized by the same number of decay vertices and charged tracks in the final state as the signal modes.

In this analysis we use 180 pb^{-1} of $p\bar{p}$ collision data at $\sqrt{s} = 1.96 \text{ TeV}$ collected by the upgraded Collider Detector (CDF II) at the Fermilab Tevatron. The components of the CDF II detector pertinent to this analysis are briefly described. A more complete description can be found elsewhere [10]. We use tracks in the pseudorapidity range $|\eta| \lesssim 1$ [11] reconstructed by a silicon microstrip vertex detector (SVX II) [12] and the Central Outer Tracker (COT) [13], which are immersed in a 1.4 T solenoidal magnetic field. The SVX II detector consists of double-sided sensors arranged in five cylindrical layers. Surrounding the SVX II is the COT, an open cell drift chamber with 96 sense wires. The integrated charge collected by each wire provides a measurement of the specific ionization (dE/dx) for charged particles, allowing a separation equivalent to 1.4 Gaussian σ between π and K for $p_T > 2 \text{ GeV}/c$. A set of planar drift chambers, located outside the calorimeters and additional steel absorbers, is used to detect muons within $|\eta| \leq 1$ with high purity.

A sample enriched with heavy flavor particles is selected by the three-level displaced track trigger. At Level 1, charged tracks are reconstructed in the COT by the eXtremely Fast Tracker (XFT) [14]. The trigger requires two oppositely charged tracks with transverse momenta $p_T \geq 2 \text{ GeV}/c$ and the scalar sum $p_{T1} + p_{T2} \geq 5.5 \text{ GeV}/c$. At Level 2, the Silicon Vertex Tracker (SVT) [15] associates SVX II r - ϕ position measurements with XFT tracks, providing a precise measurement of the track impact parameter (d_0), the distance of closest approach of the track trajectory to the beam axis in the transverse plane. Decays of heavy flavor particles are identified by requiring two tracks with $120 \mu\text{m} \leq d_0 \leq 1.0 \text{ mm}$ and an opening angle $2^\circ \leq |\Delta\phi| \leq 90^\circ$. A requirement $L_{xy} > 200 \mu\text{m}$ is also applied, where the two-dimensional decay length, L_{xy} , is calculated as the

transverse distance from the beam axis to the two track intersection projected onto the total transverse momentum of the track pair. A complete event reconstruction is performed at Level 3, where the Level 1 and Level 2 trigger requirements are confirmed.

B candidates are reconstructed by detecting $\phi \rightarrow K^+K^-$ and $J/\psi \rightarrow \mu^+\mu^-$ decays. In the latter case at least one of the muons has to be identified in the muon detectors to suppress contamination from other two-body J/ψ decays. At least one pair of tracks ("trigger tracks"), has to satisfy the trigger requirements. B^+ (B_s^0) candidates are formed by fitting three (four) tracks with $p_T > 0.4 \text{ GeV}/c$ to a common vertex. Requiring a good vertex fit χ^2 reduces background from mismeasured tracks. Combinatoric background is reduced by exploiting several variables sensitive to the long lifetime and relatively hard p_T spectrum of B mesons and the isolation of B hadrons inside b -quark jets. For this purpose we define the quantity I_R as the ratio of the B^+ candidate p_T over the total transverse momenta of all tracks within a cone of radius $R = \sqrt{\Delta\eta^2 + \Delta\phi^2} = 1$ around the B flight direction. Requiring the B flight direction to extrapolate back to the beam axis decreases background from partially reconstructed decays. The cut values on the discriminating variables are optimized by maximizing $S/\sqrt{S+B}$ for the already observed $B^+ \rightarrow \phi K^+$ signal and $S/(1.5 + \sqrt{B})$ for $B_s^0 \rightarrow \phi\phi$ whose branching ratio is unknown. The latter choice is equivalent to maximizing the potential to reach a 3σ observation of a new signal [16]. The signal (S) is derived from a Monte Carlo (MC) simulation [17] of the CDF II detector and trigger that uses the B meson momentum and rapidity distributions from Ref. [18], which were matched to CDF data. The background (B) is represented by appropriately normalized data selected with the same requirements as the signal except for the two-kaon invariant mass lying in the ϕ sideband region: $1.04 < m_{KK} < 1.06 \text{ GeV}/c^2$.

We discuss first the $B^+ \rightarrow \phi K^+$ analysis. The optimization results in the following requirements: vertex $\chi^2 < 8$, B^+ decay length $L_{xy} > 350 \mu\text{m}$, B^+ reconstructed impact parameter $d_0^B < 100 \mu\text{m}$, isolation $I_R > 0.5$, non-trigger track transverse momentum $p_T^{soft} > 1.3 \text{ GeV}/c$ and impact parameter $d_0^{soft} > 120 \mu\text{m}$.

The $B^+ \rightarrow \phi K^+$ yield and A_{CP} , defined as

$$A_{CP} \equiv \frac{N(B^- \rightarrow \phi K^-) - N(B^+ \rightarrow \phi K^+)}{N(B^- \rightarrow \phi K^-) + N(B^+ \rightarrow \phi K^+)},$$

are extracted simultaneously from an extended unbinned maximum likelihood fit on four variables: the three-kaon invariant mass (m_{KKK}), the invariant mass of the ϕ candidate (m_{KK}), the cosine of the ϕ meson helicity angle (defined as the angle between the K^+ momentum in the parent ϕ rest frame and the momentum of the ϕ in the B rest frame) and the measured dE/dx deviation from the expected value for pions for the lowest momentum trigger track. The likelihood function has seven

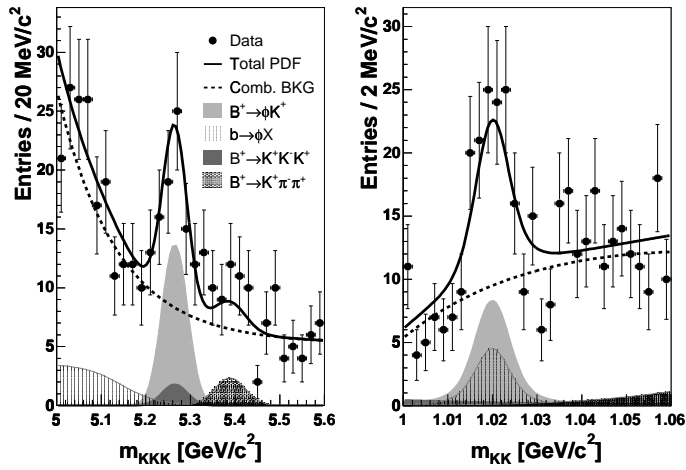


FIG. 1: m_{KKK} (left) and m_{KK} (right) distributions for $B^+ \rightarrow \phi K^+$ with projections of the likelihood function and background components described in the text.

components: signal, partially reconstructed $b \rightarrow \phi X$ decays, combinatoric background, $B^+ \rightarrow K^{*0}(892)\pi^+$, with $K^{*0} \rightarrow K^+\pi^-$, $B^+ \rightarrow f_0(980)K^+$, with $f_0 \rightarrow K^+K^-$, non-resonant $B^+ \rightarrow K^+K^-K^+$ and $B^+ \rightarrow K^+\pi^-\pi^+$. The normalizations of the last three components are fixed to the $B^+ \rightarrow K^{*0}(892)\pi^+$ yield, determined in the fit, through their relative decay rates and detection efficiencies. For each component the likelihood function is the product of four one-dimensional probability density functions (PDF) of the fit variables, which are assumed to be uncorrelated. The m_{KKK} and m_{KK} distributions are shown in Fig. 1 with projections for the different components.

A combination of Monte Carlo simulation and side-band data is used to derive the PDF in each variable for the various fit components. For m_{KKK} the fully reconstructed signals are modeled by Gaussian functions. The mass and width of the B signals are determined from the fit in the case of KKK final states, while for $K\pi\pi$ they are fixed to the values predicted by the simulation. We derive a parameterization from simulation for the partially reconstructed decays that populate the low mass side of the m_{KKK} distribution. An exponential plus a constant describe the combinatoric background. In the PDF for m_{KK} , the ϕ resonance is described by a Breit-Wigner convoluted with a Gaussian resolution function, while the combinatoric background is modeled by an empirical phase space function. Shapes for other backgrounds are derived from simulation. The ϕ helicity PDFs for B decays are derived from simulation, while the combinatoric background PDF is modeled using data from the ϕ sideband. The dE/dx PDFs for kaons and pions are derived from a high statistics $D^0 \rightarrow K^-\pi^+$ sample obtained from $D^{*\pm}$ decays. We find $N_{\phi K} = 47.0 \pm 8.4$, $A_{CP} = -0.07 \pm 0.17$ and $N_{K^{*0}\pi^+} = 7.8 \pm 6.0$ (statistical errors only) from which we estimate a $B^+ \rightarrow f_0(980)K^+$

contamination of 11% under the signal peak.

Candidates for the normalization mode, $B^+ \rightarrow J/\psi K^+$, are selected with the same requirements as the $B^+ \rightarrow \phi K^+$ candidates except for the invariant mass of the two muons being within 100 MeV/ c^2 of the J/ψ mass [8]. Using an extended likelihood fit of the $m_{\mu\mu K}$ and $m_{\mu\mu}$ distributions, we obtain a total yield of $N_{\psi K} = 439 \pm 22$ (statistical error only). The asymmetry $A_{CP}(B^+ \rightarrow J/\psi K^+) = 0.046 \pm 0.050$ is consistent with zero as expected for this mode.

The relative $B^+ \rightarrow \phi K^+$ decay rate is calculated using:

$$\frac{\text{BR}(B^+ \rightarrow \phi K^+)}{\text{BR}(B^+ \rightarrow J/\psi K^+)} = \frac{N_{\phi K}}{N_{\psi K}} \frac{\text{BR}(J/\psi \rightarrow \mu\mu)}{\text{BR}(\phi \rightarrow KK)} \frac{\epsilon_{\psi K}}{\epsilon_{\phi K}} \epsilon_{\psi K}^{\mu},$$

where $\epsilon_{\psi K}/\epsilon_{\phi K} = 0.721 \pm 0.011$ is the ratio of the combined trigger and selection efficiencies derived from MC with a correction of about 5% due to the different trigger efficiency for muons and kaons as measured in unbiased samples. The efficiency for identifying at least one of the decay muons, $\epsilon_{\psi K}^{\mu} = 0.81 \pm 0.02$, is obtained weighting the expected p_T spectra in our signal with the single muon identification efficiency measured as a function of p_T in a sample of inclusive $J/\psi \rightarrow \mu^+\mu^-$ decays. The relative $\text{BR}(B^+ \rightarrow \phi K^+)$ and A_{CP} results are reported in Table I. Systematic uncertainties on signal yield (± 1.4 events) and asymmetry ($+0.034 -0.02$) are evaluated by varying the PDFs used in the likelihood fit, including a variation of the $f_0(980)$ width from 40 to 100 MeV/ c^2 . The uncertainties on the determination of efficiency and muon identification introduce a 5.6% relative error in the measurement of the branching ratio and have no effect for A_{CP} . The uncertainties from $\text{BR}(\phi \rightarrow KK)$ and $\text{BR}(J/\psi \rightarrow \mu\mu)$ contribute an additional 2% to the total systematic. We determine a ± 0.005 uncertainty on the A_{CP} measurement arising from a possible tracking efficiency asymmetry for K^+ and K^- as measured in minimum bias data.

TABLE I: Results for $B^+ \rightarrow \phi K^+$ and $B_s^0 \rightarrow \phi\phi$ decays. World average [8] $\phi \rightarrow K^+K^-$ and $J/\psi \rightarrow \mu^+\mu^-$ BR have been used to obtain the BR ratio $\text{BR}(B^+ \rightarrow \phi K^+)/\text{BR}(B^+ \rightarrow J/\psi K^+)$ and $\text{BR}(B_s^0 \rightarrow \phi\phi)/\text{BR}(B_s^0 \rightarrow J/\psi\phi)$. The first uncertainty is statistical, the second is systematic.

	$B^+ \rightarrow \phi K^+$	$B_s^0 \rightarrow \phi\phi$
Yield	$47.0 \pm 8.4 \pm 1.4$	$7.3_{-2.5}^{+3.2} \pm 0.4$
BR ratio	$(7.6 \pm 1.3 \pm 0.6) \times 10^{-3}$	$(10_{-4}^{+5} \pm 1) \times 10^{-3}$
A_{CP}	$-0.07 \pm 0.17_{-0.02}^{+0.03}$	-

A “blind” search for $B_s^0 \rightarrow \phi\phi$ decays was performed fixing the selection requirements and evaluating the combinatoric background from independent samples before examining the signal region in the data. The signal is selected requiring two pairs of kaons having an invariant mass within 15 MeV/ c^2 of the world average ϕ mass [8].

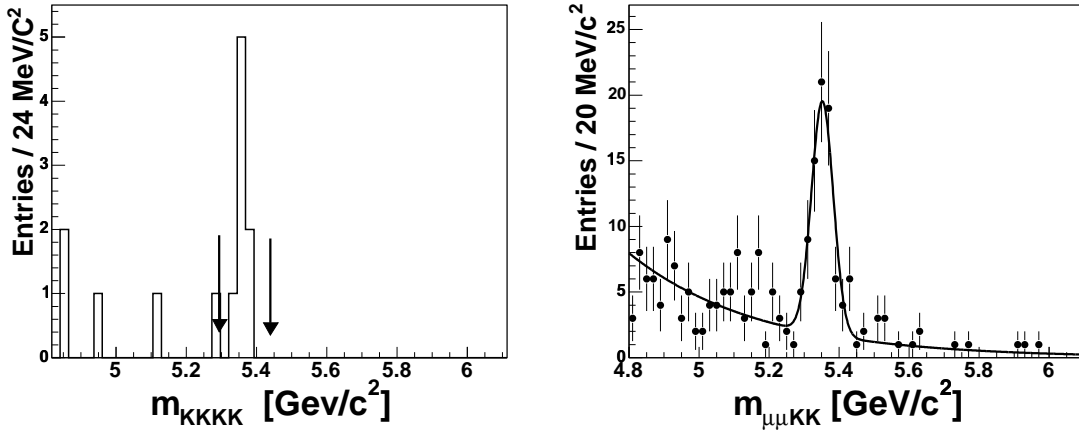


FIG. 2: Invariant mass distribution for $B_s^0 \rightarrow \phi\phi$ (left) and $B_s^0 \rightarrow J/\psi\phi$ (right) candidates. The arrows indicate the signal region for the $B_s^0 \rightarrow \phi\phi$ search. The fit described in the text is superimposed on the $m_{\mu\mu KK}$ distribution.

The optimized selection criteria are the following: vertex $\chi^2 < 10$, B_s^0 decay length $L_{xy} > 350 \mu\text{m}$, B_s^0 reconstructed impact parameter $d_0^B < 80 \mu\text{m}$, minimum ϕ meson transverse momentum $p_T^\phi > 2.5 \text{ GeV}/c$ and minimum of the two kaons' impact parameters from each ϕ meson candidate $d_{0\text{min}}^{\phi_1} > 40 \mu\text{m}$, $d_{0\text{min}}^{\phi_2} > 110 \mu\text{m}$, where ϕ_1 is the lower momentum ϕ candidate. The $B_s^0 \rightarrow \phi\phi$ candidate mass distribution is shown in Fig. 2. In a region of $\pm 72 \text{ MeV}/c^2$ around the world average [8] B_s^0 mass, corresponding to a window three times the expected mass resolution, we observe 8 events.

Two sources of background are expected in the B_s^0 signal region: combinatoric background and $B^0 \rightarrow \phi K^{*0}$ decays with the pion from the K^{*0} decay treated as a kaon. The combinatoric background generates a smooth distribution in the invariant mass region close to $m_{B_s^0}$. Its contribution in the signal region is 0.35 ± 0.37 events (combining statistical and systematic uncertainties), estimated using a background enriched sample where both ϕ meson candidates have invariant mass lying in the ϕ mass sideband region. The $B^0 \rightarrow \phi K^{*0}$ background results in an approximately Gaussian distribution underneath the B_s^0 signal. Its contribution, derived from simulation, is 0.37 ± 0.18 events where the error includes both statistical and systematic uncertainties, resulting in a signal yield of 7.3 ± 2.8 events. The probability of a Poisson fluctuation of the background to the observed or higher number of events is 1.3×10^{-6} , corresponding to 4.7σ one-sided Gaussian significance.

For the determination of $\text{BR}(B_s^0 \rightarrow \phi\phi)$, a normalization sample of $B_s^0 \rightarrow J/\psi\phi$ decays is selected requiring one pair of kaons and one pair of muons within 15 and 50 MeV/c^2 of the world average ϕ and J/ψ mass respectively. The other kinematic selection criteria are similar to the $B_s^0 \rightarrow \phi\phi$ mode. To extract the number of $B_s^0 \rightarrow J/\psi\phi$ events, the candidate invariant mass distribution, shown in Fig. 2, is fit with a binned maxi-

mum likelihood function using a Gaussian for the signal and an exponential for the background. The fit returns $N_{\psi\phi} = 69 \pm 10(\text{stat.}) \pm 5(\text{syst.})$ events, where the systematic error is evaluated using alternative background models for the low mass region where partially reconstructed B decays are expected. We subtract 3.7 ± 1.7 background events from $B^0 \rightarrow J/\psi K^{*0}$ decays, with the pion treated as a kaon, as estimated from simulation.

The $B_s^0 \rightarrow \phi\phi$ decay rate is derived from the relation:

$$\frac{\text{BR}(B_s^0 \rightarrow \phi\phi)}{\text{BR}(B_s^0 \rightarrow J/\psi\phi)} = \frac{N_{\phi\phi}}{N_{\psi\phi}} \frac{\text{BR}(J/\psi \rightarrow \mu\mu)}{\text{BR}(\phi \rightarrow KK)} \frac{\epsilon_{\psi\phi}}{\epsilon_{\phi\phi}} \epsilon_{\psi\phi}^\mu,$$

where $\epsilon_{\phi\phi}/\epsilon_{\psi\phi} = 0.821 \pm 0.015$ is derived from simulation as in the $B^+ \rightarrow \phi K^+$ case and $\epsilon_\mu = 0.92 \pm 0.05$ is obtained using the p_T spectra of the $B_s^0 \rightarrow J/\psi\phi$ signal and the muon identification efficiency curve discussed above.

The uncertainty on the $B_s^0 \rightarrow J/\psi\phi$ yield and background evaluation contribute 8% to the relative systematic error. The efficiencies significantly depend on both the polarization of the decay vector particles and the assumed value of $\Delta\Gamma_s$ since they affect the impact parameter of the decay products on which the trigger operates. We vary the longitudinal polarization of the $B_s^0 \rightarrow \phi\phi$ decay from 20% to 80%, the $B_s^0 \rightarrow J/\psi\phi$ polarization amplitudes within 1σ of the CDF measurement [20] and $\Delta\Gamma_s$ in the range $0.06 < \Delta\Gamma_s/\Gamma_s < 0.18$ to assign a relative systematic uncertainty of 4%. Summing in quadrature all contributions, we estimate a total relative systematic uncertainty on the ratio of $\text{BR}(B_s^0 \rightarrow \phi\phi)$ to $\text{BR}(B_s^0 \rightarrow J/\psi\phi)$ of 11%. To convert the ratio $\text{BR}(B_s^0 \rightarrow \phi\phi)/\text{BR}(B_s^0 \rightarrow J/\psi\phi)$ reported in Table I in a measurement of $\text{BR}(B_s^0 \rightarrow \phi\phi)$, we use $\text{BR}(B_s^0 \rightarrow J/\psi\phi) = (1.38 \pm 0.49) \times 10^{-3}$, obtained from correcting the CDF measurement [19] for the current value of f_s/f_d , the B_s^0 to B^0 production ratio [8]. We derive: $\text{BR}(B_s^0 \rightarrow \phi\phi) = (14 \text{ }^{+6}_{-5}(\text{stat.}) \pm 6(\text{syst.})) \times 10^{-6}$, where the systematic uncertainty includes a 36% contri-

bution due to the uncertainty on $\text{BR}(B_s^0 \rightarrow J/\psi\phi)$.

In summary, we have used $p\bar{p}$ collision data collected with the displaced track trigger of the CDF II detector to study two fully reconstructed $b \rightarrow s\bar{s}s$ penguin dominated B decays. Using the world average [8] $\text{BR}(B^+ \rightarrow J/\psi K^+)$ we measure: $\text{BR}(B^+ \rightarrow \phi K^+) = (7.6 \pm 1.3(\text{stat.}) \pm 0.6(\text{syst.})) \times 10^{-6}$ and $A_{CP}(B^+ \rightarrow \phi K^+) = -0.07 \pm 0.17(\text{stat.}) \pm_{-0.02}^{+0.03}(\text{syst.})$ which agree with previous measurements [8]. We find the first evidence of a charmless Vector-Vector B_s^0 decay and measure $\text{BR}(B_s^0 \rightarrow \phi\phi)$ in agreement with the estimate of Ref. [5] and the recently amended calculation in [6].

We thank the Fermilab staff and the technical staffs of the participating institutions for their vital contributions. This work was supported by the U.S. Department of Energy and National Science Foundation; the Italian Istituto Nazionale di Fisica Nucleare; the Ministry of Education, Culture, Sports, Science and Technology of Japan; the Natural Sciences and Engineering Research Council of Canada; the National Science Council of the Republic of China; the Swiss National Science Foundation; the A.P. Sloan Foundation; the Bundesministerium für Bildung und Forschung, Germany; the Korean Science and Engineering Foundation and the Korean Research Foundation; the Particle Physics and Astronomy Research Council and the Royal Society, UK; the Russian Foundation for Basic Research; the Comision Interministerial de Ciencia y Tecnologia, Spain; and in part by the European Community's Human Potential Programme under contract HPRN-CT-2002-00292, Probe for New Physics.

[1] K. Abe *et al.* [BELLE Collaboration], arXiv:hep-ex/0409049.

- [2] B. Aubert *et al.* [BABAR Collaboration], arXiv:hep-ex/0408072 and arXiv:hep-ex/0408090.
- [3] A. S. Dighe, I. Dunietz and R. Fleisher, Eur. Phys. J. **C6**, 647 (1999); D. Atwood and A. Soni, Phys. Rev. D **65**, 073018 (2002).
- [4] M. Raidal, Phys. Rev. Lett. **89**, 231803 (2002); A. Datta *et al.*, arXiv:hep-ph/0406192; submitted to Phys. Rev. D.
- [5] Y.-H. Chen *et al.*, Phys. Rev. D **59**, 074003 (1999).
- [6] X. Q. Li, G. R. Lu and Y. D. Yang, Phys. Rev. D **68**, 114015 (2003) [Erratum-ibid. D **71**, 019902 (2005)].
- [7] M. Beneke and M. Neubert, Nucl. Phys. B **675**, 333 (2003).
- [8] S. Eidelman *et al.* [Particle Data Group], Phys. Lett. B **592**, 1 (2004).
- [9] Charge conjugate decay modes are implied throughout this letter unless otherwise stated.
- [10] D. Acosta *et al.*, Phys. Rev. D **71**, 032001 (2005).
- [11] CDF II uses a cylindrical coordinate system in which ϕ is the azimuthal angle, r is the radius from the nominal beam axis, y points up and z points in the proton beam direction with the origin at the center of the detector. The transverse plane is the plane perpendicular to the z -axis.
- [12] A. Sill *et al.*, Nucl. Instrum. Meth. A **447**, 1 (2000).
- [13] T. Affolder *et al.*, Nucl. Instrum. Meth. A **526**, 249 (2004).
- [14] E.J. Thomson *et al.*, IEEE Trans. Nucl. Sci. **49**, 1063 (2002).
- [15] W. Ashmanskas *et al.*, Nucl. Instrum. Meth. A **518**, 532 (2004).
- [16] G. Punzi, eConf **C030908**, MODT002 (2003); arXiv:physics/0308063.
- [17] E. Gerchtein and M. Paulini, eConf **C0303241**, TUMT005 (2003); arXiv:physics/0306031.
- [18] M. Mangano, P. Nason and G. Ridolfi, Nucl. Phys. B **373**, 295 (1992).
- [19] F. Abe *et al.* [CDF Collaboration], Phys. Rev. D **54**, 6596 (1996).
- [20] D. Acosta *et al.* [CDF Collaboration], arXiv:hep-ex/0412057; submitted to Phys. Rev. Lett.